doi:10.1016/j.jmb.2005.02.066 J. Mol. Biol. (2005) 348, 939–949

JMB

Available online at www.sciencedirect.com

SCIENCE DIRECT®

ELSEVIER

Structural Insights into Fusidic Acid Resistance and Sensitivity in EF-G

Sebastian Hansson[1], Ranvir Singh[1], Anatoly T. Gudkov[2], Anders Liljas[1] and Derek T. Logan[1]*

[1]*Department of Molecular Biophysics, Lund University Box 124, S-221 00 Lund, Sweden*

[2]*Institute of Protein Research Russian Academy of Sciences 142290 Pushchino, Moscow Region, Russian Federation*

**Corresponding author*

Fusidic acid (FA) is a steroid antibiotic commonly used against Gram positive bacterial infections. It inhibits protein synthesis by stalling elongation factor G (EF-G) on the ribosome after translocation. A significant number of the mutations conferring strong FA resistance have been mapped at the interfaces between domains G, III and V of EF-G. However, direct information on how such mutations affect the structure has hitherto not been available. Here we present the crystal structures of two mutants of *Thermus thermophilus* EF-G, G16V and T84A, which exhibit FA hypersensitivity and resistance *in vitro*, respectively. These mutants also have higher and lower affinity for GTP respectively than wild-type EF-G. The mutations cause significant conformational changes in the switch II loop that have opposite effects on the position of a key residue, Phe90, which undergoes large conformational changes. This correlates with the importance of Phe90 in FA sensitivity reported in previous studies. These structures substantiate the importance of the domain G/domain III/domain V interfaces as a key component of the FA binding site. The mutations also cause subtle changes in the environment of the "P-loop lysine", Lys25. This led us to examine the conformation of the equivalent residue in all structures of translational GTPases, which revealed that EF-G and eEF2 form a group separate from the others and suggested that the role of Lys25 may be different in the two groups.

Keywords: protein synthesis; elongation factor G; conformational change; fusidic acid resistance; crystal structures

Introduction

The elongation phase of bacterial protein biosynthesis on the ribosome is promoted by two related GTPases, elongation factors Tu and G (EF-Tu and EF-G) which interact sequentially with the ribosome.[1,2] EF-Tu in complex with GTP and aminoacyl transfer RNA (aa-tRNA) binds with high affinity to ribosomes with an empty acceptor site (A-site), while the peptidyl site (P-site) is occupied by peptidyl tRNA carrying the growing polypeptide. Following codon–anticodon recognition, GTP hydrolysis takes place and a conformational change in EF-Tu leads to a decrease in its affinity for aa-tRNA and the ribosome.[3] As a result, EF-Tu:GDP leaves the ribosome. The peptidyl transferase reaction then occurs spontaneously and the nascent polypeptide is thereby elongated by one amino acid. Subsequently EF-G in complex with GTP catalyses the translocation step, in which the A-site tRNA carrying the nascent polypeptide and the deacylated tRNA in the P-site are moved to the P and exit (E) sites, respectively, with concomitant advance of the mRNA by one codon.[4] After GTP hydrolysis EF-G in complex with GDP dissociates from the ribosome, which is then ready for the next round of elongation. EF-G, like EF-Tu, belongs to the GTPase superfamily.[5] Both factors bind to overlapping sites on the ribosome in a sequential and mutually exclusive manner and their GTPase activities are both dramatically enhanced by ribosome binding.[6,7]

The source of all detailed structural information on EF-G to date has been the protein from *Thermus thermophilus*, which contains 691 amino acid residues and consists of six domains[8] (Figure 1(a)).

Abbreviations used: FA, fusidic acid; EF-G, EF-Tu, elongation factor G and Tu, respectively; aa-tRNA, aminoacyl transfer RNA; MPD, methane pentane diol.

E-mail address of the corresponding author: derek.logan@mbfys.lu.se

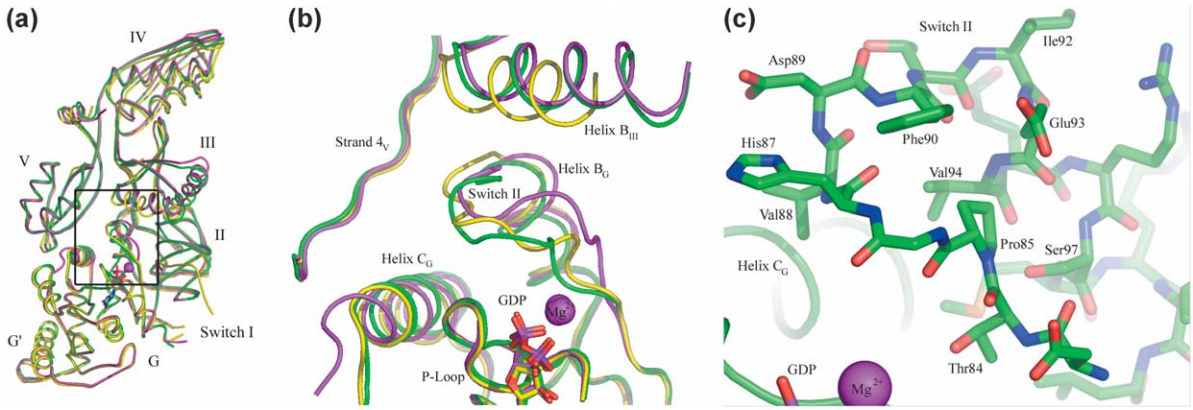

Figure 1. Comparison of EF-G structures with H573A, T84A and G16V mutations. (a) Superimposition of the C^{α} traces from H573A EF-G (green), T84A (magenta) and G16V (yellow). (b) Zoom in on the box in (a) showing the significant local differences in the conformations of switch II and helix B_{III}. The colour scheme is the same as for (a). (c) An all-atom representation of switch II in the "wild-type" conformation observed in mutant H573A. The importance of Phe90 and Pro85 for the hydrophobic core can clearly be seen. In all panels, the GDP molecules are shown in a ball-and-stick representation with carbon atoms coloured identically to the C^{α} traces. The Mg ions are shown as magenta spheres.

The structural mimicry between EF-G and EF-Tu in its ternary complex with aa-tRNA and GDPNP is striking, since the G-domain and domain II are structurally similar and domains III, IV and V of EF-G resemble the anticodon stem-loop of the tRNA.[9] The conformational changes occurring in the catalytic cycle of EF-Tu are relatively well characterized.[10,11] However, in the case of EF-G, detailed structural information is available only for the apo form and for the EF-G in complex with GDP.[8,12] The structure of EF-G:GTP is not yet known.

The elongation cycle of protein synthesis is the target of several antibiotics. Fusidic acid (FA), a potent narrow spectrum steroid antibiotic, blocks protein synthesis by inhibiting EF-G directly.[13] FA binds with high affinity to EF-G on the ribosome after GTP hydrolysis and therefore prevents the release of EF-G:GDP from the ribosome, thereby stalling protein synthesis.[14] FA has been effectively used for more than three decades in clinics against severe Gram positive infections such as those caused by certain *Staphylococcus aureus* strains.[15,16] It is an active agent against staphylococci resistant to other classes of antibiotics. Due to its effects on EF-G it has also been used as an effective tool to understand the fundamental aspects of translation.[17]

Numerous mutations in the *fusA* gene encoding EF-G conferring FA resistance have been identified and phenotypically characterized *in vivo* in *Salmonella typhimurium*[18] and in *S. aureus*.[19] The availability of the EF-G structure provided an opportunity to map these resistance mutations to give a plausible explanation of their mechanisms of action and of the binding site of FA.[8,20] The main conclusions so far can be outlined as follows. (1) Resistant mutations are spread all over EF-G, suggesting that a few mutations might be interacting directly with the FA binding site while most of them exert their effects indirectly. (2) Three distinct clusters of mutations were identified, mapping to the G domain, domain III and domain V. (3) Most likely the mutations in these clusters operate by modulating EF-G affinity for the ribosome, FA or both, and/or by restricting the conformational changes required for EF-G function.[20,21]

In our earlier efforts we have tried to explain the ways in which these clusters of mutations might exert their effect, as well as proposing a probable FA binding site.[20,22] However, in spite of the substantial information about FA resistant mutations, few such mutations have been characterized in detail *in vitro*[22–24] and there is no direct structural information available on such mutants which might explain the mechanism of action of FA in structural terms or further illuminate the location of the FA binding site on EF-G.

Here we present the crystal structures of two such mutants of EF-G from *T. thermophilus*, G16V and T84A, both in complex with GDP. Both mutants are active in poly(U)-directed translation and they hydrolyse GTP in the presence of ribosomes. They are known to confer sensitivity and resistance towards FA, respectively, and have been characterized *in vitro*.[25] The G16V mutant displays a 20 times lower K_i value for inhibition by FA of multiple rounds of GTP hydrolysis on the ribosome than does wild-type EF-G (0.4 μM *versus* 7.5 μM). The effect for the T84A mutant is the opposite: the K_i value is increased by a factor of 60, to 440 μM. These effects are correlated with GTP affinity: G16V has seven times higher affinity for GDPNP than does wild-type protein (13 μM *versus* 94 μM); T84A has four times less affinity (410 μM), while the GDP binding is not affected in either mutant.

Our results highlight the importance of switch II dynamics and structural plasticity at the interface of the G domain with domains III and V for sensitivity or resistance of EF-G to FA. Significant movements at this interface have been observed in crystal structures of EF-G[21,22] as well as in cryo-electron

microscopy (EM) studies of ribosomal complexes.[26–28] Comparable studies of the eukaryotic homologue eEF2 and eukaryotic 80 S ribosomes also show similar domain movements.[29,30] We also provide an explanation for the observed correlation between FA resistance and GTP affinity for these EF-G mutants.

Results

The space group is $P2_12_12_1$ for both mutant crystals, as in all the other reported crystal structures of EF-G.[8,12,21,22] Two types of cell dimensions have been reported for EF-G. While the *a* and *c* axes are very similar, there is a large variation in the length of the *b* axis. In the first group (wild-type EF-G with or without GDP; PDB entries 1DAR, 1EFG, 2EFG and 1ELO) *b* is ≈106 Å while mutant H573A (PDB entry 1FNM) has a significantly shorter *b* axis: *b*=86.0 Å (Table 1). This mutant also exhibits a 10° rotation of domains III, IV and V with regard to domains G and II, around an axis between domains G and V, leading to a shift of 9 Å at the tip of domain IV.[22] This more compact conformation of EF-G leads to an ordering of domain III, which is largely invisible in the other group of structures. In the following description and discussion, the crystal structure of the mutant H573A[22] will be used for comparison due to the fact that it contains an ordered domain III. Both the mutant structures discussed here are overall more similar to H573A than to wild-type EF-G, in both domain orientation and crystal packing. The differences are most likely due to the ordered binding of Mg^{2+} to GDP in the crystal forms with the shorter cell dimensions (see below). Another argument for the relevance of the H573A structure is the striking resemblance of its switch II conformation to the one observed in the crystal structure of the apo form of the eukaryotic homologue eEF2,[31] where domain III is also fully ordered. The domain movements observed between the two forms of EF-G:GDP are not in conflict with experiments on EF-G mobility involving cross-linking.[32] Besides, the H573A mutant is fully active in GTP hydrolysis and translocation.[33] Taken together, this evidence suggests that the structure of H573A:GDP is the best one for comparison to the current mutant EF-Gs.

Table 1. Crystallographic data collection and structure refinement statistics

A. *Parameters*		
EF-G mutant	T84A	G16V
Space group	$P2_12_12_1$	
Cell dimensions (Å)		
a-axis	78.2	76.3
b-axis	88.5	89.7
c-axis	116.9	114.9
Data resolution (Å)	25–2.4	28–2.6
No. observations	206, 752	213, 096
No. unique reflections	27, 567	24, 149
Completeness (overall/ outer shell) (%)	99.6/87.9	98.2/97.2
I/σ_I (overall/outer shell)	19.1/4.1	14.0/3.2
R_{merge} (%)	5.9 (41.2)	6.4 (44.7)
B. *Refinement*		
R_{model}	21.0	22.0
R_{free}	27.4	29.7
No. of non-hydrogen atoms	5289	5149
No. of water molecules	134	86
C. *rms deviations from ideal geometry*		
Bond length (Å)	0.013	0.012
Bond angles (°)	1.52	1.43
D. *Ramachandran plot (%)*		
Most favoured	90.6	87.8
Additionally allowed	8.9	10.7
Generously allowed	0.5	1.1
Disallowed	0	0.4

An overall superposition of the three structures of mutant H573A and mutants G16V and T84A is shown in Figure 1(a). The most pronounced conformational differences between the three structures are located in switch II and its surroundings. These local conformational differences cause small shifts in the relative orientations of the domains.

In H573A, switch II is located between the GDP molecule in domain G and helix B_{III} in domain III and consists of a loop region (residues 84–90) and a helix known as B_G (residues 91–100; Figure 1(b)). It is located at the interface between the P-loop, which forms part of the nucleotide-binding site in the G domain, and domains II, III and V. The residues Gly16 and Thr84 are located on β-strand 1_G and at the beginning of the switch II loop, respectively. Their C^α atoms are only 6 Å apart in space. Thr84 makes an important stabilizing interaction through its O^γ atom to the main-chain carbonyl oxygen atom of Ile17. At Gly16 there is no space for any larger residue than a glycine. The tip of switch II is stabilized by a small hydrophobic core consisting of the side-chains from one side of helix B_G (Phe90, Val94 and the aliphatic parts of Glu93 and Ser97) packing against Pro85 from the loop region (Figure 1(c)).

Switch II is rather flexible in both mutants. In SIGMAA-weighted $2m|F_o|-D|F_c|$ maps for T84A, most of the model can easily be fitted into the electron density, except for His87. This residue lacks density around its C^α and parts of the side-chain (Figure 2(a)). Density appears when the map is contoured at 0.8σ. Electron density for the backbone of switch II is clearly visible in the G16V mutant and most of the side-chains have density at a contour level of 1.0σ, except for once more that of residue His87 (Figure 2(b)). Again some density appears for this residue at a contour level of 0.8σ. However, His87 is not known as an essential residue in modulating EF-G sensitivity/resistance towards FA.

Comparison of the conformations of mutants T84A and H573A in complex with GDP

Threonine 84 is part of the conserved DtpGh motif in switch II.[5] It makes two H-bonds from its O^γ atom: one to the main-chain carbonyl of Ile17 at the end of strand 1_G of the central β-sheet (adjacent

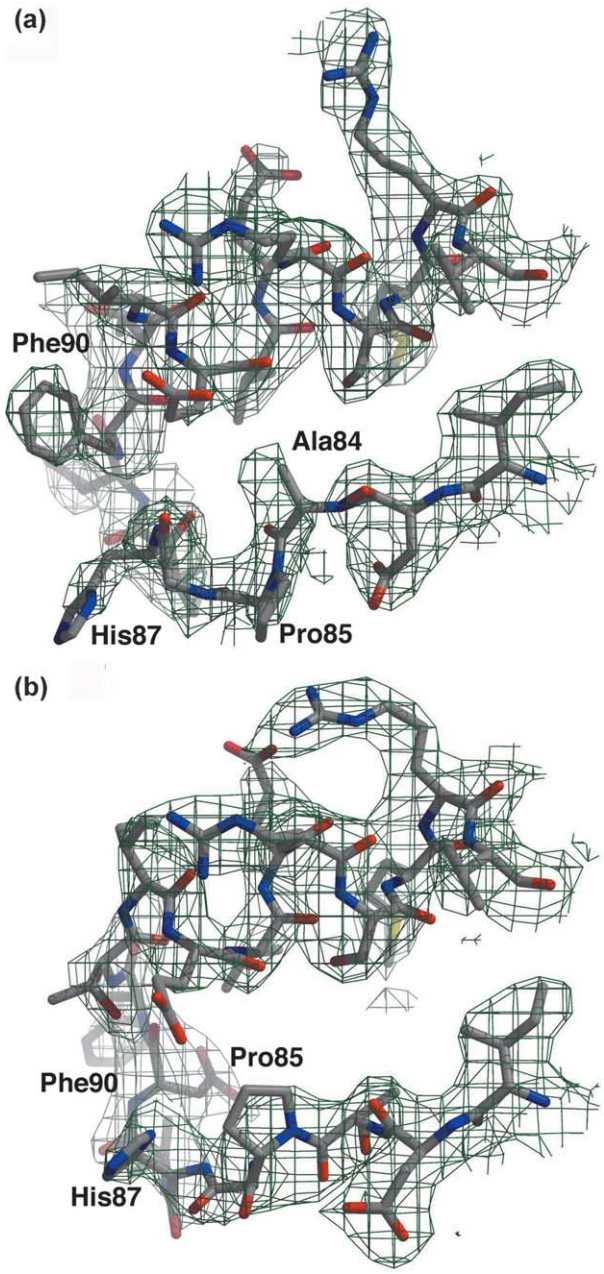

Figure 2. Electron density maps for the T84A and G16V mutants. Electron density for the switch II loop and helix (B_G) in EF-G mutants (a) T84A and (b) G16V. All atoms of the switch II region are shown in a ball-and-stick representation. The SIGMAA-weighted $2m|F_o|-D|F_c|$ maps from Refmac are shown as dark green meshes and are contoured at a level of 0.8σ above the mean.

to Gly16) and one to the side-chain of Lys25 in the P-loop. The loss of these interactions through mutation of Thr84 to Ala makes no difference to the overall conformation of either the P-loop or strand 1_G, except for a 1.5 Å movement of the tip of Lys25 towards the core of domain G (see Discussion). In contrast, the mutation has a drastic effect on the conformation of the loop region of switch II (residues 84–91). In H573A, residues 87–90 form a β-turn that projects the side-chains of His87 and Val88 towards helix C_G (Figure 3(a) and (b), green structures). Phe90 protrudes in the opposite direction and packs against Leu457 and Ile461 on helix B_{III} of domain III. In contrast, in T84A Ala84 flips upwards toward domain 3 by approximately 170° due to the loss of the H-bond to its O^{γ} atom and its C^{α} atom moves away from the central β-sheet by 4.4 Å compared to wild-type (Figure 3(c)). The hydrophobic core of switch II is disrupted due to the movement of Pro85 away from the core. The tip of switch II adopts a new conformation, in particular giving a distinct new side-chain orientation to Phe90. Phe90 no longer forms part of the switch II core but rather packs into a hydrophobic pocket formed by Leu457, His458, Ile92 and Val94, thus constituting a buttress between helix B_G of switch II (Figure 3(a)) and domain III. Both Phe90 and domain III have well-defined electron density, in contrast to mutant G16V, where domain III is more poorly ordered (see below). Helix B_G is largely unaffected by the mutation.

Apart from these local conformational changes, the overall structure of T84A is well-conserved with respect to H573A. The rms deviation between the two structures is 0.7 Å for 643 C^{α} atoms and there are no special domain movements except for those in the loop part of switch II. The lack of domain rearrangements is most likely due in part to the negligible influence of the mutation on helix B_G.

Comparison of the conformations of mutants G16V and H573A in complex with GDP

Glycine 16 is part of the conserved structural scaffold of G-proteins, situated in strand 1_G of the central β-sheet. In wild-type and H573A EF-G there is no space for residues larger than Gly at this position. In other G-proteins very few conformational changes are observed between the GDP and GTP conformations in this region.[34] An extensive mesh of contacts stabilizes the structures at this point. Residue 16 is surrounded by the side-chains of Thr84 and Leu101 of helix B_G (the switch II helix). The local effect of the G16V mutation is to break some of the interactions responsible for the conformations at the beginning and end of switch II in H573A (Figure 3(d)). In G16V Thr84 is pushed away from the central β-sheet by the side-chain of Val16, in the direction of domain III. This results in the loss of the H-bond between the O^{γ} atom of Thr84 and the carbonyl group of Ile17, similarly to mutant T84A; nevertheless in G16V the same atom maintains an H-bond to the N^{ε} atom of Lys25, due to flexibility in the latter side-chain. Otherwise there are only small differences in the P-loop that can be attributed to the mutation. The side-chain of His20 moves by roughly 1 Å and the tip of the side-chain of Lys25 moves by 1.5 Å out of the protein core (see Discussion). The G16V mutation also causes a hinge movement in helix B_G. Val16 pushes away the side-chain of Leu101, whose C^{α} atom moves by 0.6 Å. However, the movement is amplified towards the

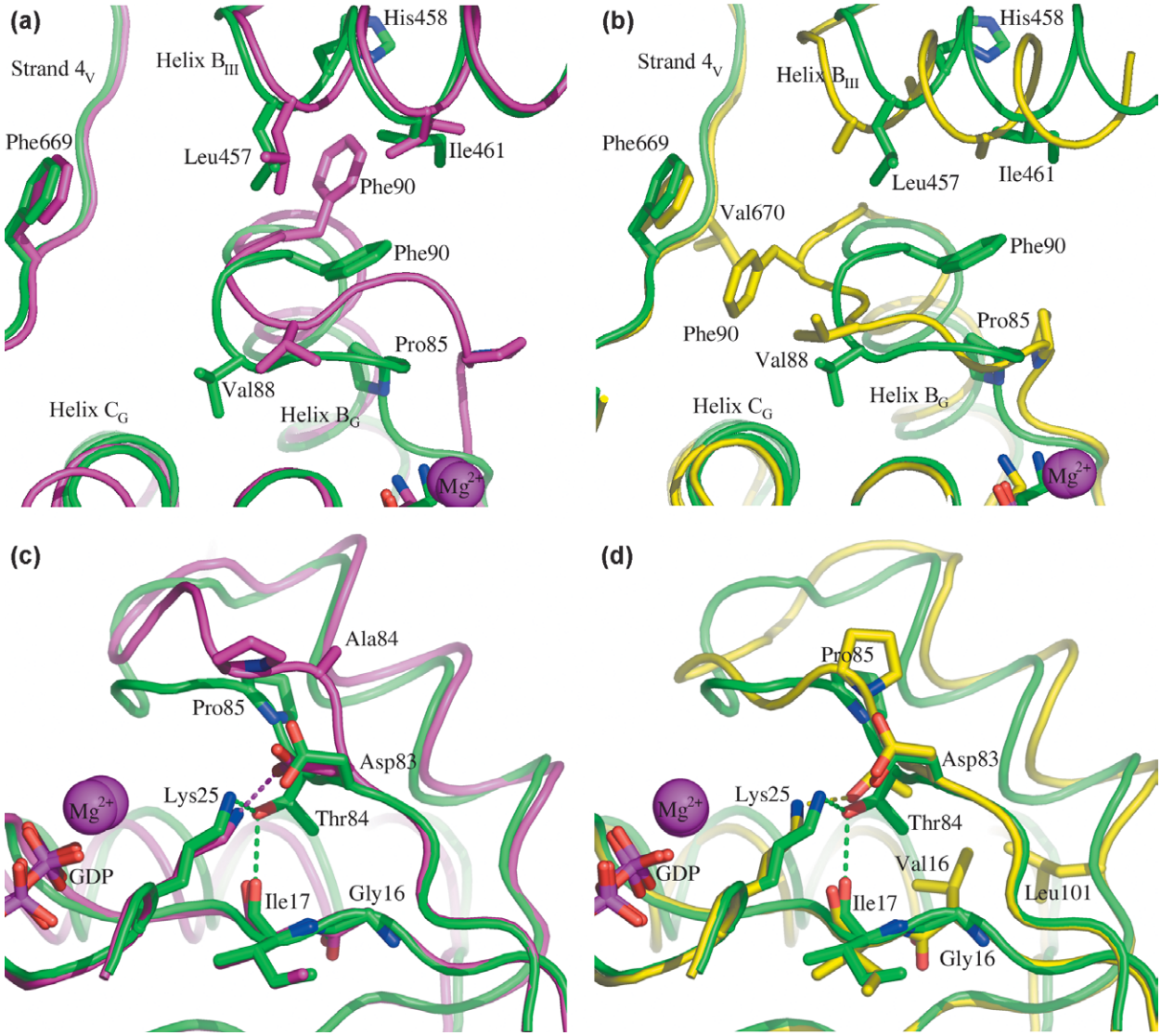

Figure 3. Important interactions and conformational changes in switch II. (a) and (b) The substantially different conformations of switch II, in particular Phe90, in EF-G mutants T84A (a), and G16V (b), which highlight the importance of Phe90 for fusidic acid resistance or sensitivity. In both panels the H573A structure is shown as in a green cartoon representation with all atoms drawn for the side-chains. Mutant T84A is drawn in magenta in (a) and mutant G16V is drawn in yellow in (b). (c) and (d) The subtle conformational changes induced in the side-chain of Lys25 by the two mutations T84A (c) and G16V (d), which suggests an explanation of the different affinities of these mutants for GTP. The molecular representations and colour coding are as for (a) and (b). In the T84A structure shown in (c) the interactions between Thr84 to both the side-chain of Lys25 and the carbonyl oxygen atom on Ile17 are lost. Pro85 loses its interaction to the hydrophobic core of switch II and Asp83 moves to compensate the stabilization of Lys25. In G16V the interaction between O^{γ} of Thr84 and the carbonyl oxygen atom of Ile17 is lost.

N-terminal end of helix B_G, with a maximum C^{α} displacement of 2.3 Å at Glu95.

The rest of switch II refolds to accommodate the changes at the beginning and end caused by the added bulk of Val16. The tip of switch II is stabilized by a set of interactions quite different from H573A or T84A. The hydrophobic core found in the H573A mutant structure is again broken, as the loop region of switch II is pushed away from the central β-sheet, causing an outward movement of Pro85. Phe90 is rotated away from domain III towards domain V, where it makes hydrophobic interactions with Ser668, Phe669 and Val670 (Figure 3(b)). This represents a third distinct conformation for Phe90, which is diametrically opposed to the conformation in T84A when both are compared to the H573A structure.

Relative to the G domain the other domains rearrange slightly. There is a hinge movement of domain II away from the central β-sheet that follows the hinge movement of helix B_G. At the extremity of domain II the C^{α} atom of Glu295 moves by as much as 2.6 Å. There is some rearrangement of the H-bonding pattern between residues Arg96 and Arg99 on the helix B_G following switch II and residues 399–400 at the end of domain II (results not shown).

The effects on domain III are more extensive. The

new conformation of switch II appears to provide less stabilization of domain III than in the H573A structure, as electron density for much of domain III is weaker in the G16V mutant despite the same compact overall conformation of EF-G. In particular helix B_{III}, (residues 456–467), which makes contacts with switch II, has indistinct side-chain electron density and has been built as poly(Ala). This helix moves significantly with respect to the G domain (Figures 1(b) and 3(b)).

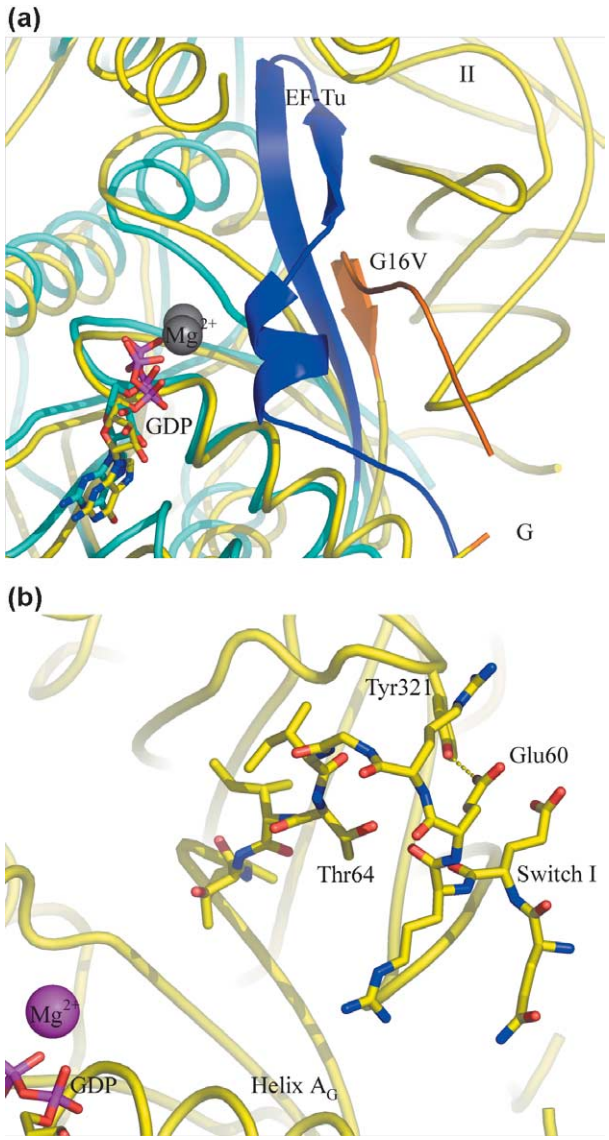

Figure 4. The newly ordered portion of switch I in mutant G16V. (a) Overall position of switch I in the GDP conformations of EF-Tu (dark blue) and EF-G G16V (orange). The remainder of these structures are shown as light blue and yellow tubes, respectively. It can clearly be seen that switch I in E-G G16V departs from its C terminus near the body of the protein in a quite different way to EF-Tu. (b) Detailed structure of the newly ordered part of switch I in G16V showing its relative position between helix A_G and domain II. The view is rotated approximately 30° anticlockwise with respect to (a). The H-bond between Glu60 and Tyr321 from domain II may help to stabilize the position of switch I. Thr64 is also labelled as reference.

Switch I and crystal packing

In H573A EF-G, switch I (the effector loop) is disordered between residues 40–65. In the original EF-G structure it is disordered between residues 39–66. Interestingly, switch I has become significantly more ordered at its C-terminal end in the G16V mutant. Residues from 57 and forward are visible, even though the *B*-factors are high (up to 86 Å^2 compared to an average of 57 Å^2 for the whole structure). It is remarkable that switch I does not reach towards domain III as it does in EF-Tu, where it helps to push away domain II of EF-Tu in its GDP conformation (Figure 4(a)). Instead it stretches down towards the N terminus of EF-G. The conformation is extended, and switch I makes no contacts with the body of EF-G except for a possible H-bond between the side-chains of Glu60 and Tyr321 in domain II (Figure 4(b)). Residues that are critical for the function of switch I in EF-Tu are found far from their positions in the GDP conformation of EF-Tu; in particular Thr64 of G16V:GDP is around 20 Å away from the equivalent Thr62 in EF-Tu:GDP. Instead, residues 62–66 of switch I run parallel with residues 295–298 of a neighbouring molecule in the crystal without making contact to them. The first visible residue in switch I, Gln57, approaches domain V of the same neighbouring molecule (Figure 5).

The reason for the ordering of switch I and for its deviation from the conformation expected from

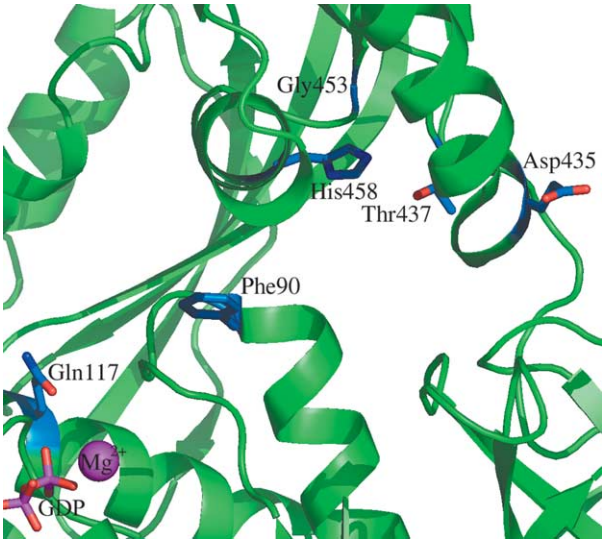

Figure 5. Mapping of the most FA resistant mutants in EF-G. A cartoon representation of the EF-G H573A structure is shown in green. The side-chains of the six most FA resistant mutations are shown in all-atom representation with carbon atoms coloured blue. In decreasing order of FA resistance, these mutations are: Phe90Leu, His458Tyr, Asp435Asn, Gln117Leu, Thr437Ile and Gly453Ser.[19] Most of these are located at or near the switch II and domain III interface.

work on EF-Tu might be explained by the presence of a crystal contact apparently induced by the presence of a Mg ion associated with GDP in the crystal structure. Domain II of a neighbouring EF-G molecule in the crystal comes close to the GDP molecule and the side-chain of Glu295 makes an H-bond to one of the water molecules coordinating the Mg^{2+}. In this conformation Tyr342 of domain II in the neighbouring molecule also makes an H-bond directly to the 2′-OH of the GDP ribose and the carbonyl oxygen atom of Gly347 H-bonds to the 2-NH_2 group of the base. Arg396 makes a salt bridge to Glu22 in the P-loop (not shown, see Laurberg *et al*.[22] for details). The resulting crystal packing is quite different from that of wild-type EF-G in complex with GDP, where ordered Mg^{2+} was not observed (PDB code 1ELO), even though it was included in the crystallization experiments, but is very similar to that in mutant H573A (PDB code 1FNM), where ordered Mg^{2+} is observed.[22]

Thus, while we cannot exclude that the ordering of switch I in the G16V mutant structure represents a biologically relevant conformation, subject to a high degree of rearrangement upon binding to the ribosome, we think it more likely that the conformation seen in the G16V mutant is due to the presence of crystal contacts and crowding around the GDP molecule, as proposed.[22]

The crystal packing in mutant T84A is very similar to that of G16V and H573A, with some subtle differences. Glu295 of the neighbouring molecule approaches the Mg^{2+} more closely than in G16V (3.0 Å *versus* 4.8 Å). Switch I is not visible between residues 40 and 67, despite the similarity in crystal packing compared to G16V, although the electron density can be seen to extend in the same direction from the C terminus at lower contour levels. The reasons for this difference are not apparent.

Discussion

The two crystal structures presented here represent the first direct evidence of the significant effects on EF-G tertiary structure that can be caused by simple point mutations. Although the structural studies have been performed on *T. thermophilus* EF-G, it is clear that they have direct relevance for EF-G in other organisms. For example, the double mutation A66V/T84A (Val69 and Thr84 in *T. thermophilus* EF-G) confers strong FA resistance upon *Escherichia coli* EF-G,[24] which has 60% sequence identity to the *T. thermophilus* factor. Since *T. thermophilus* EF-G naturally contains the Val69 residue, the T84A mutant is a close mimic of the double mutant in *E. coli*. In *S. typhimurium* an FA resistant allele of *fusA* encoding EF-G with the P413L mutation confers a slow growing phenotype and selection of resistance strains for fast growth resulted in internal revertants carrying an additional mutation along with P413L. The G13V revertant in *S. typhimurium* EF-G (also having 60% identity to *T. thermophilus*) reduces FA resistance significantly of the strain carrying the *fusA* gene with the P413L mutation.[20] Gly16 in EF-G from *T. thermophilus* corresponds to Gly13 in *S. typhimurium* EF-G. Together with the *in vitro* results for the *T. thermophilus* factor,[25] this evidence indicates that EF-G structure and function in the different organisms are highly related in their behaviour towards FA.

Mechanism of FA resistance

On the basis of structural mapping of FA resistant mutations, it has been suggested that the interface between switch II, domain III and domain V is the most likely place where FA binds.[20,22] The two mutants studied are close to the proposed FA binding site and also to the nucleotide-binding site. Thr84 is part of the DxxG consensus motif in the switch II region which is present in all G proteins.[5] This motif is generally involved in the conformational changes between the GTP and GDP states of G proteins.[35] Although it is of exclusively structural importance in EF-G, Gly16 is in close vicinity to the GTP binding site, with a distance of 10 Å between its C^{α} atom and the β-phosphate of GDP in the crystal structures.

The current work reveals two new, distinct switch II conformations in the T84A and G16V mutant structures when compared to the structure of the H753A mutant, which we use as a model for wild-type EF-G. These conformational changes result in substantial movements of the Phe90 side-chain. Phe90 is part of the small hydrophobic core that stabilizes the conformation of the tip of switch II in

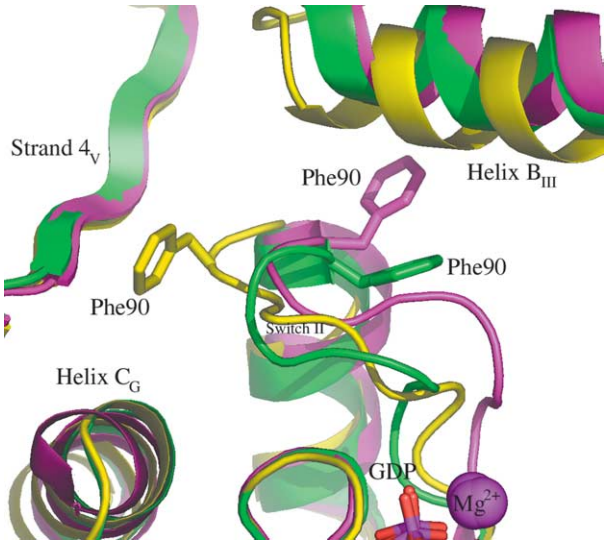

Figure 6. Comparison of the position of Phe90 in H573A, T84A and G16V. In H573A (green), Phe90 reaches into the hydrophobic pocket of switch II and is pressed down by helix B_{III} from domain III. In T84A (magenta), Phe90 reaches into the interface of switch II and helix B_{III} of domain III. Phe90 in G16V (yellow) makes a third, completely different set of interactions. It makes hydrophobic interactions with Phe669 and Val670 in domain V.

wild-type EF-G. The side-chain conformation of Phe90 in the H573A mutant structure of EF-G lies between the two extreme conformations observed in the T84A and G16V mutant structures (Figure 6). The diametrically opposite positions of the Phe90 side-chain in G16V and T84A thus appear to be correlated to their ability to confer high resistance and sensitivity towards FA, respectively. In this context it merits attention that mutation of Phe90 to Leu in *S. aureus* confers 500-fold resistance towards FA while mutations of the other two residues which flank the cavity of the proposed FA binding site, Asp435 to Asn and His458 to Tyr, both in *S. aureus*, lead to 125 and 168-fold resistance, respectively.[19,22] It is also noteworthy that the equivalent Phe111 in EF2 undergoes large conformational changes between the apo- and sordarin-bound conformations.[29]

The dramatic movement of Phe90 as observed in T84A and G16V structures is related to the "domino" effect which we proposed earlier,[22] where we suggested a possible link between the nucleotide binding and the FA binding sites. Interestingly, residues outside switch II in this domino chain (e.g. Gln117, Leu457) can also influence FA resistance when mutated.[18,22] This emphasizes the significant role of switch II and the interface between the two parts of the molecule, namely domains G and II *versus* domains III, IV and V, in fusidic acid resistance.[22] The two extreme and diametrically opposite side-chain conformations of Phe90 in the mutants represent almost the total range of available conformational space for this residue. Along with switch II, Phe90 thus appears to respond differentially to mutations, in this way regulating the gating of the possible cavity for FA binding and thus modulating the resistance of EF-G towards FA. Mutations far from this domain interface may exert their influence by relaying conformational changes to Phe90. Phe90 thus appears to be an essential residue that can partition mutations into varying degrees of resistance by its ability to adopt discrete conformational states in between the two ends of the spectrum of conformational space represented by G16V and T84A. Conformational changes associated with EF-G upon ribosome binding may further regulate the domain reorganisation, with the Phe90 sensor readjusting itself to take into account those signals. Electron microscopy reconstructions of EF-G on the ribosome in different functional states[27,36] suggest that the influence of the ribosome is most likely indirect, by facilitating a conformation of EF-G which is less favourable in solution. In any case the flexibility of Phe90 and the rest of switch II is highly likely to be an essential component of the conformational change blocked by FA.

The conformation of switch II in the original crystal structure of EF-G in complex with GDP[21] is very similar to that in the T84A mutant from Phe90 and onwards, although residues 84–89 are very different. This may appear to be in conflict with the interpretation described above; however, since domain III is largely disordered in this structure (in particular helix B_{III} is not visible) it is not possible to describe how this would affect the interactions of switch II with domain III. Nevertheless, the similarity of switch II in these two structures does confirm that this conformation of this part of switch II in T84A is an energetically stable one.

A possible role for Lys25 in affinity for GDP and GTP

Several FA resistant mutants have reduced GTP affinity and FA sensitive EF-G mutants have increased affinity for GTP.[25] Mutants T84A and G16V in solution have been reported to have four times less and three times higher affinity for GDPNP, respectively, as compared to wild-type EF-G. There thus seems to be a correlation between the FA resistance of EF-G and its affinity for GTP, though GDP binding is not affected.[25] The crystal structures of G16V and T84A presented here are in complex with GDP, thus a direct interpretation of the correlation between FA resistance of EF-G and GTP affinity is not possible. However, the structures suggest a possible explanation for this correlation that can be investigated further.

We observe subtle changes in the position of the side-chain of the "P-loop lysine", Lys25, due to the mutations, which are, as previously noted, close in space. In wild-type EF-G and in the H573A mutant, Thr84 makes an H-bond to Lys25, stabilizing its side-chain. In G16V Lys25 retains its H-bond to Thr84 but follows it towards its new position, resulting in a movement of the N^{ε} atom of Lys25 by 1.6 Å out from the core of domain G towards the supposed γ-phosphate position (Figure 3(d)). In Thr84 the H-bond between Lys25 and Thr84 is lost and is replaced by a new H-bond to the side-chain of Asp83. This has the effect that N^{ε} of Lys25 moves away from the supposed γ-phosphate position by 1.5 Å towards the core of domain G (Figure 3(c)). This suggested to us that the dynamic behaviour of Lys25 may be important for the GTPase activity of EF-G. It is known that at least one lysine residue is required for GTP binding in EF-G from *E. coli*.[37] Of the 39 lysine residues present in EF-G from *T. thermophilus*, Lys25 is almost completely conserved in all known GTPases, ATPases and even in some kinases.[38,39] It is quite excluded from the solvent in the wild-type EF-G structure and is in the vicinity of the nucleotide-binding site.

The movements observed in Lys25 and its conservation led us to examine its behaviour in the structures of other translational GTPases. EF-Tu, IF2/eIF5B, aIF2 and SelB have been characterized structurally in complex with GDP and GTP analogues.[40–44] A close comparison of these structures with those of EF-G provides insights into the possible role of the P-loop lysine (Lys24 in EF-Tu, Lys18 in IF2/eIF5B, Lys23 in aIF2 and Lys32 in eEF2). In EF-G, eEF-2 and IF2/eIF5B there is a polar residue with H-bonding possibility (Thr or Ser) at

the position equivalent to Thr84 in EF-G that can interact with the P-loop lysine. In EF-G and eEF2 the lysine is indeed hydrogen-bonded to this residue, pointing straight towards switch II and unavailable for interaction with GDP.[31] In EF-Tu, its eukaryotic and mitochondrial homologues, SelB and aIF2, there is a hydrophobic residue (Cys, Met, Val) at the position equivalent to Thr84. In the GDP complexes of these translational GTPases the P-loop lysine is bent towards the nucleotide and interacts with the β-phosphate oxygen atom;[41–45] in the corresponding GDPNP complexes the same lysine residue interacts with both the β and γ-phosphate oxygen atoms.[41–43,46] In none of the latter structures is there direct interactions between the P-loop lysine and switch II except through a water molecule. In addition, despite the presence of Thr in IF2/eIF5B, the interaction visible in EF-G between Lys25 and Thr84 is not seen between Lys18 and Thr77 in either of the IF2/eIF5B structures.[41] It thus seems that an important interaction between the P-loop lysine and the Thr or Ser of the DxxG motif in switch II is conserved in eEF2 and EF-G, but not in the other translational GTPases. This may point to differences in the way that the nucleotide-binding site is influenced by the ribosome during the catalytic cycle. The differential affinities of EF-G mutants T84A and G16V for GTP may thus be explained by the direct effect of these mutations on the environment of Lys25. However, this requires additional experiments to be clarified. Preliminary experiments indicate that the K25A mutant of *T. thermophilus* EF-G has severely reduced GTPase activity (A.T.G., unpublished results).

In conclusion, the structural studies of the two mutants presented here show that the conformation of Phe90 parallels the affinity for fusidic acid, again suggesting that the FA binding site is between domains G, III and V. In addition to the domino chain providing a signalling pathway between the nucleotide binding site and the presumed FA binding site, switch II can directly influence the environment of the nucleotide, as seen in the movements of Lys25.

Materials and Methods

Cloning, expression and purification

The gene for EF-G from *T. thermophilus* was cut out from the original pET11c vector using NdeI and EcoRI and ligated into pET13a with the same restriction sites. The site-directed mutagenesis was performed using QuickChange XL II (Stratagene®). The primers used for G16V were forward 5′-CTCCGGAACATCGT CATCGCCGCCC and reverse 5′-GGGCGGCGATGAC GATGTTCCGGAG; for T84A the forward primer was 5′-AACATCATCGACGCCCCGGGCCACG and reverse 5′-CGTGGCCCGGGGCGTCGATGATGAA. Expression and purification of both the mutants, were performed as described[47] with slight modifications. Heat denaturing treatment of post-ribosomal supernatant was carried out at 70 °C for 15 minutes for coagulation of *E. coli* proteins. Coagulated proteins were removed by centrifugation and the supernatant was applied to a Source 15Q anion exchange column (AmershamBiosciences®). EF-G was eluted with a gradient from 0 M to 1 M NaCl in a buffer containing 60 mM Tris–HCl (pH 7.6), 5 mM β-mercapto-ethanol, 1 mM EDTA and 0.1 mM PMSF. Protein obtained after anion exchange chromatography was pure enough to yield good quality crystals. All protein solutions were concentrated in crystallization buffer containing 5 mM Tris–HCl, 10 mM $MgCl_2$ (pH 7.6) to a concentration of 3–4 mg/ml.

Crystallization

The crystallization buffer for T84A and G16V was 5 mM Tris–HCl (pH 7.6), 10 mM $MgCl_2$ and 5 mM GDP (Sigma®). Crystals of T84A:GDP and G16V:GDP were grown from hanging drops in vapour diffusion experiments at pH 7.3 against 17% (w/v) polyethylene glycol 8000 (Fluka®), 100 mM Hepes and 46 mM Tris; 4 μl of a 4 mg/ml protein solution was mixed with 4 μl of reservoir solution. The G16V and T84A drops were initially streak seeded with wild-type EF-G crystals but in later experiments crystals of the respective mutants were used. Good quality crystals of both mutants appeared overnight and were of suitable size for data collections (0.4 mm × 0.4 mm × 0.2 mm). Crystals were passed rapidly through a drop with conditions identical with the crystallization drops but with the addition of 49% methane pentane diol (MPD) as cryo-protectant, from which they were transferred directly into the liquid nitrogen cryo stream. The T84A:GDP and G16V:GDP crystals appeared to be more fragile than wild-type EF-G and the use of glycerol as cryo-protectant was not suitable, therefore MPD was used instead.

Data collection and structure determination

Diffraction data for T84A:GDP were collected to 2.4 Å resolution on a 165 mm MarCCD detector at station I711 of the Max-II synchrotron, Lund, Sweden and the G16V:GDP data were collected to 2.6 Å resolution on an ADSC Q4R CCD detector at station ID14-EH1 of the ESRF, Grenoble, France. All data were collected at 100 K. The data were integrated with XDS.[48] All data were further processed with programs from the CCP4 suite[49] using the CCP4i interface.[50] The T84A:GDP structure was solved using the structure of the H573A mutant, Protein Data Bank (PDB) entry 1FNM[22] as search model in the molecular replacement program Molrep.[51] The G16V:GDP structure was solved using T84A:GDP as search model. Both models were rebuilt using XtalView[52] and refined with Refmac5[53] (Table 1). Figures were made using Pymol† except for Figure 3, which was made using Bobscript.[54] Structural superimpositions were made using SwissPDB Viewer.

Coordinates

Coordinates and structure factors have been deposited in the RCSB Protein Data Bank[55] with accession numbers 2BM1 for the G16V mutant and 2BM0 for the T84A mutant.

† http://www.pymol.org.

Acknowledgements

This work was supported by grants from the Swedish Research Council (to V.R.), the Crafoord Foundation, Carl Tryggers Foundation and the Royal Swedish Academy of Sciences (to D.L.), a grant from VR and EU grant QLK2-CT-2002-00892 (to A.L.), and in part by Russian grant 02-04-48953 from RFBR (to A.T.G.). We thank staff at MAX-lab (Y. Cerenius) and beamline ID14 of the ESRF (in particular C. Romão) for help with data collection.

References

1. Nishizuka, Y. & Lipmann, F. (1966). Comparison of guanosine triphosphate split and polypeptide synthesis with a purified *E. coli* system. *Proc. Natl Acad. Sci. USA*, **55**, 212–219.
2. Richman, N. & Bodley, J. W. (1972). Ribosomes cannot interact simultaneously with elongation factors EF-Tu and EF-G. *Proc. Natl Acad. Sci. USA*, **69**, 686–689.
3. Krab, I. M. & Parmeggiani, A. (1998). EF-Tu, a GTPase odyssey. *Biochim. Biophys. Acta*, **1443**, 1–22.
4. Rodnina, M. V., Savelsbergh, A. & Wintermeyer, W. (1999). Dynamics of translation on the ribosome: molecular mechanics of translocation. *FEMS Microbiol. Rev.* **23**, 317–333.
5. Bourne, H. R., Sanders, D. A. & McCormick, F. (1991). The GTPase superfamily: conserved structure and molecular mechanism. *Nature*, **349**, 117–127.
6. Richter, D. (1972). Inability of *E. coli* ribosomes to interact simultaneously with the bacterial elongation factors EF-Tu and EF-G. *Biochem. Biophys. Res. Commun.* **46**, 1850–1856.
7. Miller, D. L. (1972). Elongation factors EF Tu and EF G interact at related sites on ribosomes. *Proc. Natl Acad. Sci. USA*, **69**, 752–755.
8. Ævarsson, A., Brazhnikov, E., Garber, M., Zheltonosova, J., Chirgadze, Y., Al-Karadaghi, S. *et al*. (1994). Three-dimensional structure of the ribosomal translocase: elongation factor G from *Thermus thermophilus*. *EMBO J.* **13**, 3669–3677.
9. Liljas, A. (1996). Imprinting through molecular mimicry. Protein synthesis. *Curr. Biol.* **6**, 247–249.
10. Polekhina, G., Thirup, S., Kjeldgaard, M., Nissen, P., Lippmann, C. & Nyborg, J. (1996). Helix unwinding in the effector region of elongation factor EF-Tu-GDP. *Structure*, **4**, 1141–1151.
11. Abel, K., Yoder, M. D., Hilgenfeld, R. & Jurnak, F. (1996). An alpha to beta conformational switch in EF-Tu. *Structure*, **4**, 1153–1159.
12. Czworkowski, J., Wang, J., Steitz, T. A. & Moore, P. B. (1994). The crystal structure of elongation factor G complexed with GDP, at 2.7 Å resolution. *EMBO J.* **13**, 3661–3668.
13. Tanaka, N., Kinoshita, T. & Masukawa, H. (1968). Mechanism of protein synthesis inhibition by fusidic acid and related antibiotics. *Biochem. Biophys. Res. Commun.* **30**, 278–283.
14. Bodley, J. W., Zieve, F. J., Lin, L. & Zieve, S. T. (1969). Formation of the ribosome-G factor-GDP complex in the presence of fusidic acid. *Biochem. Biophys. Res. Commun.* **37**, 437–443.
15. Whitby, M. (1999). Fusidic acid in the treatment of methicillin-resistant *Staphylococcus aureus*. *Int. J. Antimicrob. Agents*, **12**(Suppl 2), S67–S71.
16. Whitby, M. (1999). Fusidic acid in septicaemia and endocarditis. *Int. J. Antimicrob. Agents*, **12**(Suppl 2), S17–S22.
17. Czworkowski, J. & Moore, P. B. (1996). The elongation phase of protein synthesis. *Prog. Nucl. Acid Res. Mol. Biol.* **54**, 293–332.
18. Johanson, U. & Hughes, D. (1994). Fusidic acid-resistant mutants define three regions in elongation factor G of *Salmonella typhimurium*. *Gene*, **143**, 55–59.
19. Nagaev, I., Bjorkman, J., Andersson, D. I. & Hughes, D. (2001). Biological cost and compensatory evolution in fusidic acid-resistant *Staphylococcus aureus*. *Mol. Microbiol.* **40**, 433–439.
20. Johanson, U., Aevarsson, A., Liljas, A. & Hughes, D. (1996). The dynamic structure of EF-G studied by fusidic acid resistance and internal revertants. *J. Mol. Biol.* **258**, 420–432.
21. Al-Karadaghi, S., Ævarsson, A., Garber, M., Zheltonosova, J. & Liljas, A. (1996). The structure of elongation factor G in complex with GDP: conformational flexibility and nucleotide exchange. *Structure*, **4**, 555–565.
22. Laurberg, M., Kristensen, O., Martemyanov, K. A., Gudkov, A. T., Nagaev, I., Hughes, D. & Liljas, A. (2000). Structure of a mutant EF-G reveals domain III and possibly the fusidic acid binding site. *J. Mol. Biol.* **303**, 593–603.
23. MacVanin, M., Johanson, U., Ehrenberg, M. & Hughes, D. (2000). Fusidic acid-resistant EF-G perturbs the accumulation of ppGpp. *Mol. Microbiol.* **37**, 98–107.
24. Richter Dahlfors, A. A. & Kurland, C. G. (1990). Novel mutants of elongation factor G. *J. Mol. Biol.* **215**, 549–557.
25. Martemyanov, K. A., Liljas, A., Yarunin, A. S. & Gudkov, A. T. (2001). Mutations in the G-domain of elongation factor G from *Thermus thermophilus* affect both its interaction with GTP and fusidic acid. *J. Biol. Chem.* **276**, 28774–28778.
26. Agrawal, R. K., Penczek, P., Grassucci, R. A. & Frank, J. (1998). Visualization of elongation factor G on the *Escherichia coli* 70 S ribosome: the mechanism of translocation. *Proc. Natl Acad. Sci. USA*, **95**, 6134–6138.
27. Valle, M., Zavialov, A., Sengupta, J., Rawat, U., Ehrenberg, M. & Frank, J. (2003). Locking and unlocking of ribosomal motions. *Cell*, **114**, 123–134.
28. Stark, H., Rodnina, M. V., Wieden, H. J., van Heel, M. & Wintermeyer, W. (2000). Large-scale movement of elongation factor G and extensive conformational change of the ribosome during translocation. *Cell*, **100**, 301–309.
29. Jorgensen, R., Ortiz, P. A., Carr-Schmid, A., Nissen, P., Kinzy, T. G. & Andersen, G. R. (2003). Two crystal structures demonstrate large coonformational changes in the eukaryotic ribosomal translocase. *Nature*, **10**, 379–385.
30. Spahn, C. M., Gomez-Lorenzo, M. G., Grassucci, R. A., Jorgensen, R., Andersen, G. R., Beckmann, R. *et al*. (2004). Domain movements of elongation factor eEF2 and the eukaryotic 80 S ribosome facilitate tRNA translocation. *EMBO J.* **23**, 1008–1019.
31. Jorgensen, R., Yates, S. P., Teal, D. J., Nilsson, J., Prentice, G. A., Merrill, A. R. & Andersen, G. R. (2004). Crystal structure of ADP-ribosylated ribosomal translocase from *Saccharomyces cerevisiae*. *J. Biol. Chem.* **279**, 45919–45925.
32. Peske, F., Matassova, N. B., Savelsbergh, A., Rodnina, M. V. & Wintermeyer, W. (2000). Conformationally

restricted elongation factor G retains GTPase activity but is inactive in translocation on the ribosome. *Mol. Cell*, **6**, 501–505.
33. Martemyanov, K. A., Yarunin, A. S., Liljas, A. & Gudkov, A. T. (1998). An intact conformation at the tip of elongation factor G domain IV is functionally important. *FEBS Letters*, **434**, 205–208.
34. Vetter, I. R. & Wittinghofer, A. (2001). The guanine nucleotide-binding switch in three dimensions. *Science*, **294**, 1299–1304.
35. Kjeldgaard, M., Nyborg, J. & Clark, B. F. (1996). The GTP binding motif: variations on a theme. *FASEB J.* **10**, 1347–1368.
36. Agrawal, R. K., Linde, J., Sengupta, J., Nierhaus, K. H. & Frank, J. (2001). Localization of L11 protein on the ribosome and elucidation of its involvement in EF-G-dependent translocation. *J. Mol. Biol.* **311**, 777–787.
37. Giovane, A., Balestrieri, C. & Gualerzi, C. (1982). Structure–function relationships in *Escherichia coli* translational elongation factor G: modification of lysine residues by the site-specific reagent pyridoxal phosphate. *Biochemistry*, **21**, 5224–5230.
38. Saraste, M., Sibbald, P. R. & Wittinghofer, A. (1990). The P-loop–a common motif in ATP- and GTP-binding proteins. *Trends Biochem. Sci.* **15**, 430–434.
39. Leipe, D. D., Wolf, Y. I., Koonin, E. V. & Aravind, L. (2002). Classification and evolution of P-loop GTPases and related ATPases. *J. Mol. Biol.* **317**, 41–72.
40. Krab, I. M. & Parmeggiani, A. (2002). Mechanisms of EF-Tu, a pioneer GTPase. *Prog. Nucl. Acid Res. Mol. Biol.* **71**, 513–551.
41. Roll-Mecak, A., Cao, C., Dever, T. E. & Burley, S. K. (2000). X-ray structures of the universal translation initiation factor IF2/eIF5B: conformational changes on GDP and GTP binding. *Cell*, **103**, 781–792.
42. Schmitt, E., Blanquet, S. & Mechulam, Y. (2002). The large subunit of initiation factor aIF2 is a close structural homologue of elongation factors. *EMBO J.* **21**, 1821–1832.
43. Leibundgut, M., Frick, C., Thanbichler, M., Bock, A. & Ban, N. (2005). Selenocysteine tRNA-specific elongation factor SelB is a structural chimaera of elongation and initiation factors. *EMBO J.* **24**, 11–22.
44. Andersen, G. R., Thirup, S., Spremulli, L. L. & Nyborg, J. (2000). High resolution crystal structure of bovine mitochondrial EF-Tu in complex with GDP. *J. Mol. Biol.* **297**, 421–436.
45. Berchtold, H., Reshetnikova, L., Reiser, C. O., Schirmer, N. K., Sprinzl, M. & Hilgenfeld, R. (1993). Crystal structure of active elongation factor Tu reveals major domain rearrangements. *Nature*, **365**, 126–132.
46. Nissen, P., Kjeldgaard, M., Thirup, S., Polekhina, G., Reshetnikova, L., Clark, B. F. & Nyborg, J. (1995). Crystal structure of the ternary complex of Phe-tRNA^{Phe}, EF-Tu, and a GTP analog. *Science*, **270**, 1464–1472.
47. Martemyanov, K. A., Liljas, A. & Gudkov, A. T. (2000). Extremely thermostable elongation factor G from *Aquifex aeolicus*: cloning, expression, purification, and characterization in a heterologous translation system. *Protein Expr. Purif.* **18**, 257–261.
48. Kabsch, W. (1993). Automatic processing of rotation diffraction data from crystals of initially unknown symmetry and cell constants. *J. Appl. Crystallog.* **26**, 795–800.
49. Collaborative Computational Project, No. 4. (1994). The CCP4 suite: programs for protein crystallography. *Acta Crystallog. sect. D*, **50**, 760–763.
50. Potterton, E., Briggs, P., Turkenburg, M. & Dodson, E. (2003). A graphical user interface to the CCP4 program suite. *Acta Crystallog. sect. D: Biol. Crystallog.* **59**, 1131–1137.
51. Vagin, A. & Teplyakov, A. (2000). An approach to multi-copy search in molecular replacement. *Acta Crystallog. sect. D: Biol. Crystallog.* **56**, 1622–1624.
52. McRee, D. E. (1999). XtalView/Xfit—a versatile program for manipulating atomic coordinates and electron density. *J. Struct. Biol.* **125**, 156–165.
53. Murshudov, G. N. (1997). Refinement of macromolecular structures by the maximum-likelihood method. *Acta Crystallog. sect. D: Biol. Crystallog.* **53**, 240–255.
54. Esnouf, R. M. (1997). An extensively modified version of MolScript that includes greatly enhanced coloring capabilities. *J. Mol. Graph. Model.* **15**, 132–134 see also pp. 112–113.
55. Berman, H. M., Westbrook, J., Feng, Z., Gilliland, G., Bhat, T. N., Weissig, H. *et al*. (2000). The Protein Data Bank. *Nucl. Acids Res.* **28**, 235–242.

Edited by J. Doudna

(Received 23 December 2004; received in revised form 25 February 2005; accepted 27 February 2005)